Controlling the Microstructure and Phase Behavior of Confined Soft Colloids by Active Interaction Switching

Arturo Moncho-Jordá[1,2,*] and Joachim Dzubiella[3,4,†]

[1]Departamento de Física Aplicada, Universidad de Granada, Campus Fuentenueva S/N, 18071 Granada, Spain
[2]Instituto Carlos I de Física Teórica y Computacional, Universidad de Granada, Campus Fuentenueva S/N, 18071 Granada, Spain
[3]Applied Theoretical Physics-Computational Physics, Physikalisches Institut, Albert-Ludwigs-Universität Freiburg, Hermann-Herder Straße 3, D-79104 Freiburg, Germany
[4]Cluster of Excellence livMatS @ FIT—Freiburg Center for Interactive Materials and Bioinspired Technologies, Albert-Ludwigs-Universität Freiburg, Georges-Köhler-Allee 105, D-79110 Freiburg, Germany

(Received 10 April 2020; accepted 16 July 2020; published 10 August 2020)

We explore the microstructure and phase behavior of confined soft colloids which can *actively* switch their interactions at a predefined kinetic rate. For this, we employ a reactive dynamical density-functional theory and study the effect of a two-state switching of the size of colloids interacting with a Gaussian pair potential in the nonequilibrium steady state. The switching rate interpolates between a near-equilibrium binary mixture at low rates and a nonequilibrium monodisperse liquid for large rates, strongly affecting the one-body density profiles, adsorption, and pressure at confining walls. Importantly, we show that sufficiently fast switching impedes the phase separation of an (in equilibrium) unstable liquid, allowing the control of the degree of mixing and condensation and local microstructuring in a cellular confinement by tuning the switching rate.

DOI: 10.1103/PhysRevLett.125.078001

Active matter systems have drawn the attention of the soft matter scientific community in recent years due to their very rich dynamic behavior. They are composed by individual particles, each of which consumes energy in order to move, react, or to produce mechanical forces. Prominent examples of active soft matter systems are self-propelled nanoparticles, contracting biopolymers such as proteins or actin filaments inside the cytoskeleton, biological cells and bacteria [1–7], or synthetic active hydrogels [8–10] and vesicles [11,12]. Fascinating new dynamics have been revealed; for example, self-propelling activity has been shown to lead to motility-induced swarming, jamming, or phase separation [13,14].

Biological activity, in particular mediated through fuel-driven changes of molecular properties and conformations, has been made responsible for liquid-liquid phase separation and condensation in cells, with large implications for physiology and disease [15,16]. Living cells contain distinct subcompartments to facilitate spatiotemporal regulation of biochemical reactions where transient microstructuring is key for function. Those biology-inspired, nonequilibrium transient morphologies bear potential for the design of novel adaptive materials [17], e.g., by harvesting switchable self-assembly and structuring [9]. The microscopic origins and features of nonequilibrium structuring, however, are not well understood. Theoretical frameworks for interacting reaction-diffusion systems have been linked so far only to microstructuring dynamics of nonactive systems driven by chemical reactions [18–21] or virus infections [22]. However, activity-controlled structuring, demixing and condensation in confinement by switching microscopic conformations (and resulting interactions) has not been addressed so far.

In this Letter, in contrast to the well-studied motile activity [13,14], we investigate the effects of active conformational switching of particles on the liquid microstructuring in confinement, such as a wall or a cellular compartment. For this, we employ a reactive dynamical density functional theory (R-DDFT) put forward in other flavors previously [18–21] and apply it to the binary switching of the size of soft, interacting colloids. The latter serve as a generic model for polymers and soft colloidal hydrogels [23,24] and cells [25], where size is used as the simplest interaction variable to describe a conformational change. We show that the system then interpolates between an equilibrium binary mixture at low switching rates and a nonequilibrium monodisperse system for large rates. As a consequence, the variation of the rate substantially modifies the microstructure and phase separation of the active liquid in confinements. Hence, we demonstrate that active interaction switching dynamically controls the demixing, condensation, and local microstructuring in compartmentalized situations.

As a simple model system, mimicking, e.g., soft active hydrogels or vesicles switching (or "breathing") between two states [8–11] or responsive, conformationally switching biopolymers [4,7,15], we employ repulsive soft particles that can actively switch between two states "big" (b) and "small" (s) which differ in particle size. The interactions are

defined by repulsive Gaussian pair potentials [26], $\beta u_{ij}(r) = \epsilon_{ij} e^{-r^2/\sigma_{ij}^2}$ $(i, j = s, b)$, where r is the interparticle distance, $\beta = 1/(k_B T)$ the inverse thermal energy, $\epsilon_{ij} > 0$ the interaction strength, and σ_{ij} represents their size (we denote σ_{bb} and σ_{ss} by σ_b and σ_s, respectively). Gaussian potentials are appropriate to describe polymers and soft colloids [23,27]. A benefit is that one- and two-component Gaussian systems are well understood in and out of equilibrium and the mean-field free energy functional in DFT is quasiexact for these systems [28–33].

We emphasize that this model is actually a one-component colloidal system, but since every individual particle has two states (b and s), every microstate and also average (steady-state) distributions have to be described as for a binary mixture. We denote N_b and N_s as the number of repulsive Gaussian particles of type b and s inside a volume V, at fixed temperature T. The instantaneous bulk number density of both species are given by $\rho_i = N_i/V$ $(i = b,\ s)$. We denote the total (conserved) number density by $\rho_T = \rho_b + \rho_s = \text{const}$, and define a concentration ratio by $x = x_s = \rho_s/\rho_T$. The total volume fraction of particles is $\phi_T = \phi_b + \phi_s = (\pi/6)(\rho_b \sigma_b^3 + \rho_s \sigma_s^3)$. Nonequilibrium switching activity implies that particles of type b can be converted into s at a rate k_{bs} (units of time^{-1}). Conversely, particles of type s convert into b at a rate k_{sb}. This elementary "chemical" reaction process is ruled by the set of first-order differential equations [34]

$$d\rho_b/dt = k_{sb}\rho_s - k_{bs}\rho_b, \quad d\rho_s/dt = k_{bs}\rho_b - k_{sb}\rho_s. \quad (1)$$

The integration of these equations leads to exponential decaying time-dependent concentrations [35]. In particular, the equilibrium composition achieved in the limit $t \to \infty$ satisfies $\rho_{s,\infty}/\rho_{b,\infty} = x_\infty/(1 - x_\infty) = k_{bs}/k_{sb}$, where $\rho_{i,\infty}$ are the equilibrium densities.

In order to calculate the effect of the switching rate on the average (steady-state) liquid microstructure under a confining external potential $u_i^{\text{ext}}(\mathbf{r})$ $(i = b, s)$ we make use of classical DDFT [36,37], which successfully described the overdamped out-of-equilibrium dynamics of various soft matter systems in external potentials [38–40], including Gaussian colloids [31–33] and the action of motile activity [41–43]. Here, we extend the DDFT formulation to active mixtures in which each component switches into the other at some fixed rate, so the time evolution of the particle concentrations $\rho_i(\mathbf{r}, t)$ is not only due to the diffusive fluxes, but also to the position-dependent production and disappearance of each component following the switching. Analogous to related DDFT-based reaction-diffusion approaches [19–22], the governing reactive DDFT (R-DDFT) equations read

$$\begin{cases} \frac{\partial \rho_b(\mathbf{r},t)}{\partial t} = -\nabla \cdot \mathbf{J}_b + k_{sb}\rho_s(\mathbf{r}, t) - k_{bs}\rho_b(\mathbf{r}, t) \\ \frac{\partial \rho_s(\mathbf{r},t)}{\partial t} = -\nabla \cdot \mathbf{J}_s + k_{bs}\rho_b(\mathbf{r}, t) - k_{sb}\rho_s(\mathbf{r}, t) \end{cases}, \quad (2)$$

where $\mathbf{J}_i = -D_i[\nabla\rho_i + \rho_i \nabla\beta(u_i^{\text{ext}} + \mu_i^{\text{ex}})]$ $(i = b,\ s)$ are the diffusive fluxes, $D_i = k_B T/(3\pi\eta\sigma_i)$ are the diffusion constants of both species, and $\mu_i^{\text{ex}}(\mathbf{r}, t) = \delta F_{\text{ex}}[\{\rho_i(\mathbf{r}, t)\}]/\delta\rho_i(\mathbf{r}, t)$ are the functional derivatives of the equilibrium excess free energy functional, evaluated using the nonequilibrium density profiles, $\rho_i(\mathbf{r}, t)$ [36,37]. Since Gaussian particles behave as a weakly correlated mean-field fluid over a surprisingly wide density and temperature range [28], we use the mean-field excess functional $F_{\text{ex}} = \frac{1}{2}\sum_{i,j=b,s} \iint \rho_i(\mathbf{r}, t)\rho_j(\mathbf{r}', t)u_{ij}(|\mathbf{r} - \mathbf{r}'|)d\mathbf{r}d\mathbf{r}'$. Details about the boundary conditions and numerical integration are shown in the Supplemental Material [35].

As first applications we investigate emblematic inhomogeneous situations in confining potentials, namely, the liquid structuring at a single hard wall and the phase separation in a cellular confinement, in which the kinetic rate constants k_{bs} and k_{sb} for active switching fulfill the condition $k_{bs}/k_{sb} = x/(1 - x)$. In this way, reference bulk concentrations remain unaltered, but the inhomogeneous properties suffer the effect of the switching. We define the normalized switching rate, or *switching activity* as $a = k_{bs}\sigma_s^2/D_s$. For $a \ll 1$, the b⇌s conversion rate is so slow that the time evolution of the density profiles is dominated by diffusive equilibration, being faster than the transformative changes. It is easy to see from Eq. (2) that the steady state $(\partial\rho_i/\partial t = 0)$ then essentially reduces to the situation of a binary mixture in equilibrium. Conversely, for $a \gg 1$ the exchange rate is so large that the diffusion is not fast enough to "smear out" local activity effects, so the activity dominates the structure. In this limit, we will demonstrate that the systems behave in the steady-state as a nonequilibrium monodisperse system of same interaction size.

Table I specifies the interaction parameters and particle concentrations for three systems (S1 to S3). S1 and S2 are inside the stable region of the phase diagram, whereas S3 is located in the unstable region, so it undergoes a fluid-fluid demixing in equilibrium. For all cases, we study the final steady state for active systems from $a = 0$ (nonactive equilibrium) to large activities $a = 10^4$.

We first investigate the role that switching activity plays on the structure and adsorption of the liquid at a hard wall. We show in Figs. 1(a) and 1(b) the final steady state for different active systems from $a = 0$ to $a = 10^4$ (for the nonequilibrium relaxation from a nonsteady state, see Ref. [35]). These results show that the equilibrium density

TABLE I. Interaction parameters and concentrations for the three investigated systems. S1 and S2 are stable, whereas system S3 is unstable (demixing) in equilibrium.

System	ϵ_{bb}	ϵ_{ss}	ϵ_{bs}	σ_b/σ_s	σ_{bs}/σ_s	$\rho_T\sigma_s^3$	ϕ_T	x	k_{bs}/k_{sb}
S1	2	2	2	2	1.5	0.239	0.3	0.8	4
S2	2	2	2	2	1.5	0.191	0.45	0.5	1
S3	2	2	1.888	1.504	1.277	2.4	2.765	0.5	1

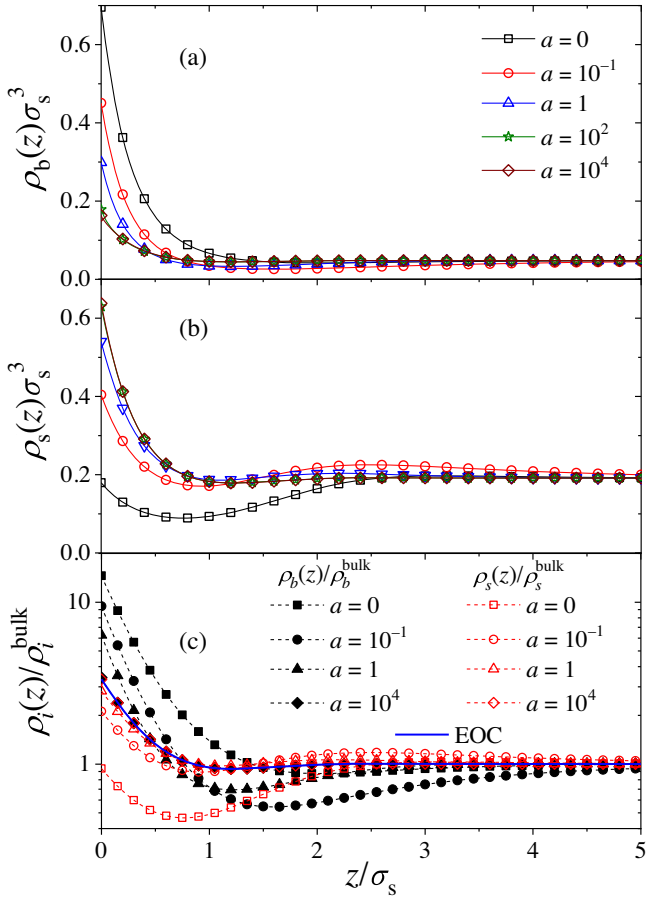

FIG. 1. Steady-state density profile of (a) big and (b) small particles (system S1) near a hard wall for different values of the activity, from $a = 0$ (nonactive) to $a = 10^4$. (c) Normalized steady-state profiles, $\rho_i(z)/\rho_i^{\rm bulk}$, of big and small particles converge to the same form for $a \to \infty$, described by the equilibrium profile of an effective one-component (EOC) system interacting with $u_{\rm eff}(r)$ given in Eq. (3).

profiles ($a = 0$) near the wall experience a considerable change even for relatively small values of the activity [$\rho_s(z)$ significantly raises up for $a = 0.1$]. Increasing the value of a entails a progressive desorption of big colloids from the wall and an enhanced adsorption of small ones. Importantly, for growing $a \gg 1$ the system tends to a steady state in which the density profiles of both components converge to each other. This trend is confirmed in Fig. 1(c), where the normalized density profiles $\rho_i(z)/\rho_i^{\rm bulk}$ of both components are depicted for increasing a. For $a \gtrsim 10^2$ both curves converge to a common average profile. In other words, in the limit of large switching activity, the system is fully monodisperse. In fact, evaluating Eq. (2) in the limit $a \to \infty$ [35] under the mean-field approximation, we obtain analytical forms for the effective interaction potential, $u_{\rm eff}(r)$, of an effective one-component system (EOC) in equilibrium whose structure is equivalent to that of the nonequilibrium monodisperse system,

$$u_{\rm eff}(r) = \frac{\sum_{i,j=b,s}(D_i + D_j)x_i x_j u_{ij}(r)}{2\sum_{i=b,s} D_i x_i}, \tag{3}$$

constituted by weighted means of the individual pair potentials (where $x_s = x$ and $x_b = 1 - x$). Using the effective potentials in equilibrium DFT of the EOC we can indeed match the nonequilibrium profiles at high rates, cf. Figs. 1(c). Interestingly, the effective potentials depend on the particle diffusivities, reflecting the nonequilibrium origin in their derivation. This behavior for $a \to \infty$ is an intrinsic property of the switching liquid and also holds in bulk, see Ref. [35] and as we will show below.

Activity also has important repercussions on the wall osmotic pressure in the active steady state. Figure 2(a) displays $\beta P_{\rm wall}\sigma_s^3 = \rho_T(0)\sigma_s^3$ as a function of a for systems S1 and S2. Both systems exactly satisfy the contact wall theorem for $a = 0$, i.e., the pressure at the wall agrees with the bulk pressure $\beta P_{\rm bulk} = \rho_T + \frac{1}{2}\rho_T^2\pi^{3/2}\sum_{i,j} x_i x_j \epsilon_{ij}\sigma_{ij}^3$. However, increasing a yields a systematic departure from this behavior, as the pressure at the wall decreases monotonically until it reaches an asymptotic limit for $a \to \infty$, described by the equilibrium pressure of an EOC interacting with effective potentials Eq. (3). Consequently, active interaction switching tunes the bulk pressure. The corresponding reduced adsorption of both components, defined as $\Gamma_i' = \int_0^\infty (\rho_i(z)/\rho_i^{\rm bulk} - 1)dz$, is depicted in Fig. 2(b). The behavior of big and small particles is very different for nonactive systems, as $\Gamma_b' > 0$ (adsorption to the wall) and $\Gamma_s' < 0$ (depletion from the wall) for $a = 0$. However, the difference between Γ_b' and Γ_s' substantially decreases for increasing rate a, whereas already for $a > 0.03$ they converge to a common value according to the monodisperse behavior.

All these results can be rationalized as follows: If $a \ll 1$ the switching events are rare and the diffusive fluxes are still able to preserve the distinction between both components. However, for $a \gg 1$ many switching effects occur during the characteristic diffusive time $\tau_0 = \sigma_s^2/D_s$, so particles do not have enough time to rearrange by diffusion, and they tend to experience the same effective interparticle interaction given by Eq. (3).

These arguments suggest that activity should also affect the inhomogeneous distribution of an equilibrium phase-separated mixture, which we consider in the following. We select a mixture with $\epsilon_{bb} = \epsilon_{ss} = 2$, $\epsilon_{bs} = 1.888$, $\sigma_b = 1.504\sigma_s$, and $\sigma_{bs} = 1.277\sigma_s$. This choice of interaction parameters corresponds to a system that undergoes fluid-fluid demixing above the critical point, located at $\rho_T^*\sigma_s^3 = 1.647$ and $x^* = 0.7$ [28,30]. We chose a total number density of $\rho_T\sigma_s^3 = 2.4$ and $x = 0.5$, which is located well inside the unstable region (system S3). The mixture is confined inside a spherical cavity (cell) of radius $R = 5\sigma_s$ [32,33]. Confinement is attained through repulsive external potentials given by $\beta u_i^{\rm ext}(r) = E_i(r/R)^{10}$ for $r \le R$ and $\beta u_i^{\rm ext}(r) = \infty$ for $r > R$, with $E_b = E_s = 20$.

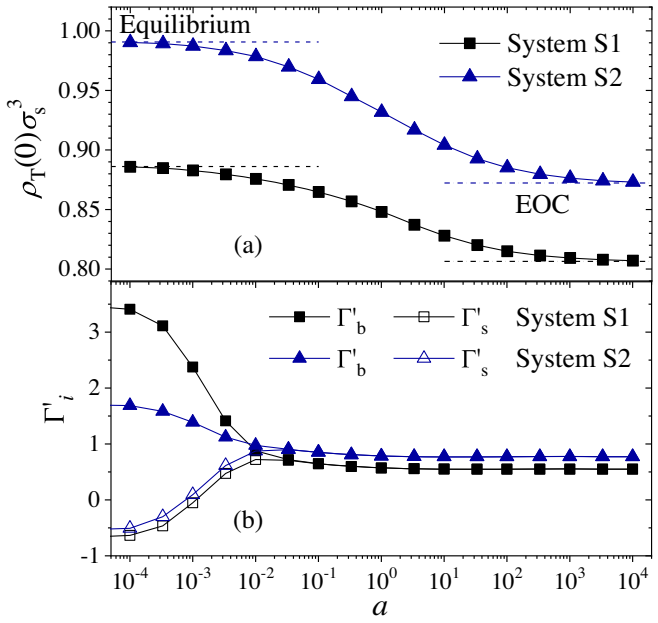

FIG. 2. (a) Pressure exerted by systems S1 and S2 onto a hard planar wall versus a in the steady state. Dashed horizontal lines indicate the bulk pressure for $a = 0$ (left side) and the equilibrium pressure of an EOC interacting with $u_{\text{eff}}(r)$ as in Eq. (3) valid for $a \to \infty$ (right side). (b) Reduced adsorption of big and small particles onto the wall versus a. ■ (system S1), ▲ (system S2).

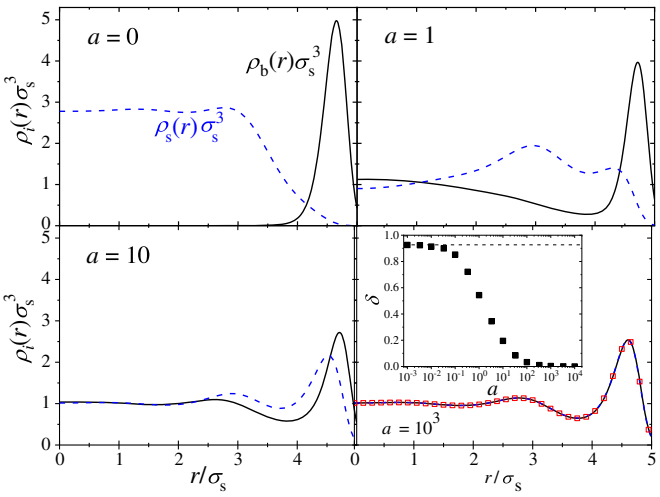

FIG. 3. Steady-state density profiles for system S3 confined inside a spherical cavity (cell) of radius $R = 5\sigma_s$, for activities from $a = 0$ to 10^3. For $a = 0$ the system is in equilibrium and demixed. Increasing a suppresses the phase separation and induces mixing. Red symbols □ represent the profile for the EOC interacting with the potential given in Eq. (3). Inset: demixing order parameter δ as a function of a.

The top-left plot of Fig. 3 shows the equilibrium ($a = 0$) density profiles for system S3, clearly exhibiting fluid-fluid phase separation in the cavity. Big particles are adsorbed or "condensed" close to the external wall of the cavity, whereas small ones are mainly distributed in the central region. This segregation is caused by the effective depletion attraction between the big particles and the wall induced by the smaller component [44]. The degree of separation between both components can be quantified by means of the demixing order parameter, defined as $\delta = \{[4\pi]/[xN_b + (1-x)N_s]\} \int_0^R |x\rho_b(r) - (1-x)\rho_s(r)|r^2 dr$, $\delta = 1$ implies that big and small particles completely demix into two nonoverlapping regions, whereas $\delta = 0$ means complete mixing. For $a = 0$, we find $\delta = 0.93$, indicating a high degree of demixing.

The steady-state profiles for larger activities are depicted in the other panels of Fig. 3 up to $a = 10^3$ (for details about the time evolution see Ref. [35]). $\rho_b(r)$ in the center of the cavity increases progressively with activity, while the height of the adsorption peak decreases. Conversely, $\rho_s(r)$ reduces in the central region, narrowing the depletion layer of small spheres around the wall while propagating interesting intermediate peaks. In other words, increasing a induces an activity-driven mixing and modified microstructuring of both components. For activities above $a = 1$, both density profiles approach each other, and for large $a > 10^2$ they converge to the result obtained with the EOC system in equilibrium, that is, demonstrate complete mixing. The transition from a phase separated to a mixed fluid is clearly recognized in the inset of Fig. 3, where δ plotted as a function of the activity tends to full mixing, $\delta \to 0$, for $a \to \infty$. This transition is gradual and centered at $a = 1$, which represents the inflection point separating mixed and demixed states. These results suggest that switching activity is a potential tool to dynamically control the demixing state of mixtures.

Finally, in order to check also how activity modifies the *intrinsic* structure of a phase-separating mixture (system S3) *in bulk*, we combine the R-DDFT, Eq. (2), with the test-particle route [45] (details in Ref. [35]). Figure 4 shows the resulting number-number structure factor, $S_{NN}(q) = 1 + \rho_T \sum_{i,j} x_i x_j \hat{h}_{ij}(q)$, where $\hat{h}_{ij}(q)$ are the

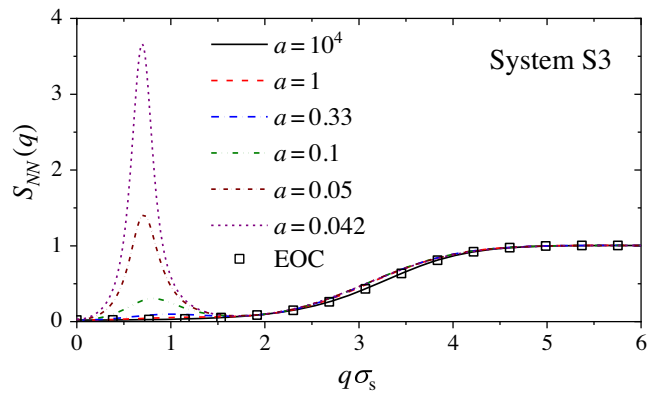

FIG. 4. Structure factor $S_{NN}(q)$ for different values of a for system S3 in bulk. The symbols □ represent the equilibrium structure of the EOC interacting with effective potential Eq. (3).

Fourier transforms of the pair distribution functions $h_{ij}(r) = g_{ij}(r) - 1$. For large a, the switching rate prevents phase separation of the mixture, and $S_{NN}(q)$ corresponds to the stable EOC, according to potential Eq. (3). However, for $a < 1$ a peak appears at low q, which grows as a decreases and shifts to smaller q values (larger wavelengths). For $a = 0.042$, this peak reaches a significant height, indicating the onset of phase separation and the development of spatially extended microclusters. These results corroborate that demixing of the intrinsic liquid (no external potential) is dynamically regulated by switching activity.

In summary, we demonstrated that active switching of particle interactions has profound effects on the inhomogeneous microstructure of colloidal suspensions. In particular, increasing activity suppresses the phase separation of in-equilibrium unstable systems inside a cellular confinement, inducing a gradual mixing of the two components. This effect may be exploited for a nonequilibrium control of the degree of demixing and have implications for liquid-liquid phase separation, condensation, and transient microstructuring in biological and synthetic functional cells [15,16] or nonequilibrium material design [9,10,17]. Our model is idealized but we believe the qualitative effects of interaction switching to be robust across different systems and interactions, as can be rationalized generally from the analytical slow and fast switching limits. As possible simple experimental realizations, we believe active colloidal hydrogels [8] or vesicles [11,12] are appropriate (where active size switching can be induced by chemical background reactions or active cytoskeleton dynamics), or, alternatively, well-defined solutions of proteins with actively (fuel-driven) switching conformations [5].

The authors thank Upayan Baul for useful discussions. J. D. has received funding from the European Research Council (ERC) under the European Union's Horizon 2020 research and innovation programme (Grant Agreement No. 646659). A. M.-J. thanks the program Visiting Scholars funded by the University of Granada (Project No. PPVS2018-08).

*moncho@ugr.es
†joachim.dzubiella@physik.uni-freiburg.de

[1] S. Ramaswamy, Annu. Rev. Condens. Matter Phys. **1**, 323 (2010).
[2] T. Sanchez, D. T. N. Chen, S. J. DeCamp, M. Heymann, and Z. Dogic, Nature (London) **491**, 431 (2012).
[3] J. Prost, F. Juelicher, and J.-F. Joanny, Nat. Phys. **11**, 111 (2015).
[4] U. B. Choi, J. J. McCann, K. R. Weninger, and M. E. Bowen, Structure **19**, 566 (2011).
[5] J.-H. Ha and S. N. Loh, Chem. Eur. J. **18**, 7984 (2012).
[6] M. C. Marchetti, J. F. Joanny, S. Ramaswamy, T. B. Liverpool, J. Prost, M. Rao, and R. A. Simha, Rev. Mod. Phys. **85**, 1143 (2013).
[7] S. Dhiman, A. Jain, and S. J. George, Angew. Chem., Int. Ed. Engl. **56**, 1329 (2017).
[8] R. Yoshida, T. Takahashi, T. Yamaguchi, and H. Ichijo, J. Am. Chem. Soc. **118**, 5134 (1996).
[9] T. Heuser, E. Weyandt, and A. Walther, Angew. Chem., Int. Ed. Engl. **54**, 13258 (2015).
[10] L. Heinen, T. Heuser, A. Steinschulte, and A. Walther, Nano Lett. **17**, 4989 (2017).
[11] H. Che, S. Cao, and J. C. M. van Hest, J. Am. Chem. Soc. **140**, 5356 (2018).
[12] Y. Bashirzadeh and A. P. Liu, Soft Matter **15**, 8425 (2019).
[13] M. E. Cates and J. Tailleur, Annu. Rev. Condens. Matter Phys. **6**, 219 (2015).
[14] C. Bechinger, R. Di Leonardo, H. Löwen, C. Reichhardt, G. Volpe, and G. Volpe, Rev. Mod. Phys. **88**, 045006 (2016).
[15] Y. Shin and C. P. Brangwynne, Science **357**, aaf4382 (2017).
[16] J. Berry, C. P. Brangwynne, and M. Haataja, Rep. Prog. Phys. **81**, 046601 (2018).
[17] A. Walther, Adv. Mater. **32**, 1905111 (2019).
[18] S. C. Glotzer, E. A. Di Marzio, and M. Muthukumar, Phys. Rev. Lett. **74**, 2034 (1995).
[19] J. F. Lutsko and G. Nicolis, Soft Matter **12**, 93 (2016).
[20] H. M. Al-Saedi, A. J. Archer, and J. Ward, Phys. Rev. E **98**, 022407 (2018).
[21] Y. Liu and H. Liu, AIChE J. **66**, e16824 (2020).
[22] M. te Vrugt, J. Bickmann, and R. Wittkowski, arXiv:2003.13967.
[23] A. A. Louis, P. G. Bolhuis, J. P. Hansen, and E. J. Meijer, Phys. Rev. Lett. **85**, 2522 (2000).
[24] A. Scotti, S. Bochenek, M. Brugnoni, M. A. Fernandez-Rodriguez, M. F. Schulte, J. E. Houston, A. P. H. Gelissen, I. I. Potemkin, L. Isa, and W. Richtering, Nat. Commun. **10**, 1418 (2019).
[25] R. G. Winkler, D. A. Fedosov, and G. Gompper, Curr. Opin. Colloid Interface Sci. **19**, 594 (2014).
[26] F. H. Stillinger, J. Chem. Phys. **65**, 3968 (1976).
[27] P. G. Bolhuis, A. A. Louis, J. P. Hansen, and E. J. Meijer, J. Chem. Phys. **114**, 4296 (2001).
[28] A. A. Louis, P. G. Bolhuis, and J. P. Hansen, Phys. Rev. E **62**, 7961 (2000).
[29] A. Lang, C. N. Likos, M. Watzlawek, and H. Löwen, J. Phys. Condens. Matter **12**, 5087 (2000).
[30] A. J. Archer and R. Evans, Phys. Rev. E **64**, 041501 (2001).
[31] J. Dzubiella and C. N. Likos, J. Phys. Condens. Matter **15**, L147 (2003).
[32] A. J. Archer, J. Phys. Condens. Matter **17**, 1405 (2005).
[33] A. J. Archer, J. Phys. Condens. Matter **17**, S3253 (2005).
[34] K. A. Dill and S. Bromberg, *Molecular Driving Forces: Statistical Thermodynamics in Chemistry and Biology* (Garland Science, New York, 2003).
[35] See Supplemental Material at http://link.aps.org/supplemental/10.1103/PhysRevLett.125.078001 for detailed derivations of the kinetic rate equations, R-DDFT equations, calculation of the time-dependent density profiles and radial distribution functions, and for the derivation of the effective one-component interparticle pair potential, $u_{\text{eff}}(r)$.

[36] U. M. B. Marconi and P. Tarazona, J. Chem. Phys. **110**, 8032 (1999).
[37] A. J. Archer and R. Evans, J. Chem. Phys. **121**, 4246 (2004).
[38] M. Rauscher, *Dynamic Density Functional Theory (DDFT)* (Springer, Boston, MA, 2013), pp. 1–8.
[39] S. Angioletti-Uberti, M. Ballauff, and J. Dzubiella, Mol. Phys. **116**, 3154 (2018).
[40] A. Moncho-Jordá, A. Germán-Bellod, S. Angioletti-Uberti, I. Adroher-Bentíez, and J. Dzubiella, ACS Nano **13**, 1603 (2019).
[41] H. H. Wensink and H. Löwen, Phys. Rev. E **78**, 031409 (2008).
[42] R. Wittkowski and H. Löwen, Mol. Phys. **109**, 2935 (2011).
[43] M. Enculescu and H. Stark, Phys. Rev. Lett. **107**, 058301 (2011).
[44] A. J. Archer and R. Evans, J. Phys. Condens. Matter **14**, 1131 (2002).
[45] J.-P. Hansen and I. McDonald, *Theory of Simple Liquids*, 4th ed. (Academic Press, New York, 2013).